Vol. xx, No. x (202x) x-x, doi:

Proceedings on Engineering Sciences

www.pesjournal.net

Sample-based Dynamic Hierarchical Transformer with Layer and Head Flexibility via Contextual Bandit

Fanfei Meng[1]
Lele Zhang[2]
Yu Chen[2]
Yuxin Wang[1]
1. Department of Electrical and Computer Engineering, Northwestern University, Evanston, 60208, IL, United States
2. Inistitute of Computing Technology, Chinese Academy of Science, Beijing, 100190, China

Keywords:

AutoML; Network Compression; Transformer and Deep Learning

A B S T R A C T

Transformer requires a fixed number of layers and heads which makes them inflexible to the complexity of individual samples and expensive in training and inference. To address this, we propose a sample-based Dynamic Hierarchical Transformer (DHT) model whose layers and heads can be dynamically configured with single data samples via solving contextual bandit problems. To determine the number of layers and heads, we use the Uniform Confidence Bound while we deploy combinatorial Thompson Sampling in order to select specific head combinations given their number. Different from previous work that focuses on compressing trained networks for inference only, DHT is not only advantageous for adaptively optimizing the underlying network architecture during training but also has a flexible network for efficient inference. To the best of our knowledge, this is the first comprehensive data-driven dynamic transformer without any additional auxiliary neural networks that implement the dynamic system. According to the experiment results, we achieve up to 74% computational savings for both training and inference with a minimal loss of accuracy

1. INTRODUCTION

These are instructions Transformers have demonstrated significant success in various linguistic tasks, including text classification [1,2], machine translation [3,4], and knowledge graphs [5]. These achievements are attributed to the powerful multi-head attention, which projects sequential tokens into parallel attention subspaces at relatively low memory and computational costs. Following the transformer framework, BERT [6] and GPT-3 [7,8] are proposed to train specific linguistic tasks using pre-trained weights. Although transformers are powerful in various aspects, it is still difficult to embed such a large network into mobile devices constrained by limited power and memory, and standard transformer is still expensive in both training and inference. Furthermore, traditional network compression methods require a full layer training firstly and then reduce the model size through layer-wise network compression [9–11] or knowledge distillation [12–14]. On the one hand, this two-step compression procedure can be of high time complexity. On the other

Corresponding author: Name Surname (Times New Roman 8pt)
Email: active email adress

hand, different tasks may require different light-weight transformers making the uniform compression inflexible. Therefore, we would like to design a dynamic, data-driven transformer model whose size can be optimized during training, skipping the separate compression step while maintaining a decent predicting capability.

Inspired by neural architecture search (NAS) and network compression [15–18], we propose a sample-based Dynamic Hierarchical Transformer (DHT) to bring dynamics to both layers and heads and formulate an adaptive network routine for every data sample. Instead of highly complex neuron-based NAS, we shed light on searching for self-attention space and limit the maximum search space by first obtaining the number of layers needed for a sample, and then moving forward to prune heads layer-by-layer to further reduce the network size. In order to determine the configurations of layers and heads for each sample in a realtime fashion, we integrate Uniform Confidence Bound multi-arm contextual bandits (UCB) [19] and Thompson Sampling semi-bandits (TSP) [20] into our DHT model, where the UCBs are responsible for determining the number of layers as well as the number of heads to keep in each layer, and the TSB the combination of heads to keep in each layer. A very unique aspect of our approach is the fact that the underlying layers and heads are sample specific, exploiting the strategy that customizes the number of layers and heads for each single sample. In addition, considering the effect of head interactions and the order samples appear during training, our work formulate rewards of batch level rather than one step gains, which successfully mitigates model performance reductions. The major contribution of our model is that it alleviates researchers in deep learning from fine-tuning transformer configurations by learning to fine-tune them automatically. Specifically, (i) our work designed a dynamic transformer model that may have different, customized number of layers, number of heads, or head combinations for each individual sample to reduce model size and training time, while maintaining good predicting performance; (ii) our work pioneered a new transformer training mechanism by adopting UCB to determine the optimal number of layers and heads and adopting TSB to select at each layer the optimal head combination for a given sample; (iii) our work study the effect of different subsets of transformer heads, while former approaches, to the best of our knowledge, merely study the effect of each individual head, lacking a more holistic observation on multi-head attention pruning that we achieve.

The structure of this paper is as follows. First, our work lists existing work similar to ours and compares how our work is distinct from them in Section 1. We further introduce in Section 2 two algorithms upon which our methodology is founded. Then, our work introduce our methodology in Section 3 and describe its implementation in Section 4. After that, our work explains the experiments we perform, and show and analyzes the result in Section 5. Lastly, our work summarizes this work in Section 6.

2. RELATED WORK

Network size compression research is progressing at an exhilarating pace. Some offer inspiring insights of applying compression to multiple deep models [12,21–26], while others dynamically compress layers using knowledge distillation and network compression for efficient inference [27–30]. With respect to transformers, network quantization is developed while imposing specific bandwidth precision compatibility for devices [31,32]. The role of each head is revealed and the semantic and syntax functions for each corresponding sample are visualized [33], allowing the development of a head pruning method based on head importance score metrics [34]. Furthermore, work has been done to shed light on linguistic representations of different heads and employ differential L_0 normalization to dynamically prune the heads [35].

In addition to the head pruning strategy, there are methods focusing on explaining attention dynamics. One work illustrates similarities among heads to learn an optimal attention span for controlling the computational time [36]. Following this work, another explores the deployment of deep Q-learning to achieve a dynamic attention span [37]. Moreover, adaptive depth of transformers is investigated, where the layer depth is determined step-by-step [38].

Sample-based architecture trainings [39–41] are investigated for improving training effects by adaptively tackling the complexity of each sample. One work reveals the variance of a data sample in model training [42]. Following this work, another tests the effect of each sample in back-propagation, and reveals that the learning effect of a single sample varies for the whole network even when the same learning rate is used [43]. Inspired by the experiment, dynamic, sample-based learning rate is proposed to train networks more effectively, where the loss is used to optimize the learning rate [44]. All these works lay foundations for our sample-based implementation. However, in addition to the training loss, we also utilize such model configuration information as the number of model layers and number of heads at each layer. Such information serves as reward factors that help decide the best model configuration for efficient training and inference by enabling adaptive underlying network updates. Furthermore, our work takes a more comprehensive approach to multi-head attention pruning, as the research studies the effect of head combinations instead of the effect of individual ones.

3. BACKGROUND

In this section, our paragraph describes the two algorithms that serve as the foundation for our methodology: Uniform Confidence Bound and Thompson Sampling Semi-Bandits.

3.1 Uniform Confidence Bound

Contextual bandit is used to find the actions for d-dimensional input samples $x=\{\mathbf{x}_1,\ldots,\mathbf{x}_n\} \in R^d$ given a finite arm set $\mathbf{Z}$. The aggregated vector corresponding to arm γ with arm feature vector $\mathbf{z}_\gamma$ is constructed as $\mathbf{w}_{i,\gamma} = [\mathbf{x}_i ; \mathbf{z}_\gamma] \in R^{2d}$ (for simplicity we assume that both have dimension d). The aggregated vector corresponding to arm γ with arm feature vector $\mathbf{z}_\gamma$ is constructed as $\mathbf{w}_{k,\gamma} = [\mathbf{x}_k ; \mathbf{z}_\gamma]$. The expected reward $r_{k,\gamma}$ with trainable $\boldsymbol{\theta}_\gamma \in R^{2d}$ is defined as follows (Li et al., 2010):

$$E[r_{k,\gamma}|\mathbf{w}_{k,\gamma}] = \mathbf{w}^T\boldsymbol{\theta}_\gamma \quad (1)$$

Let $\mathbf{D}_{i,\gamma} \in R^{k\times 2d}$ be the design matrix reflecting prior k sample i and $\mathbf{C}_{i,\gamma}, \in R^{k\times 2d}$ be the reward matrix obtained from the previous observations. Following regression the optimal parameters $\theta_{i,r}$ read

$$\boldsymbol{\theta}_{i,\gamma} = (\mathbf{D}^{T}{}_{i\gamma}\mathbf{D}_{i,\gamma} + \lambda\mathbf{I})^{-1}\mathbf{D}^{T}{}_{i,\gamma}\mathbf{C}_{i,\gamma}, \quad (2)$$

where λ is the ridge regularization factor. We summarize UCB contextual bandit in Algorithm 1.

Algorithm 1: UCB Contextual Bandit

Input: $\mathcal{X} = \{\mathbf{x}_1, \ldots, \mathbf{x}_n\}$
Initialize: $\mathbf{A}_\gamma \leftarrow \lambda \mathbf{I}_{d\times d}$, $\mathbf{b}_\gamma \leftarrow \mathbf{0}_{d\times 1}$ for each arm γ
for $i = 1, \ldots, n$ **do**
  Observe features of all arms $\gamma \in \mathcal{Z}$ and obtain $\mathbf{w}_{i,\gamma}$;
  for *each arm* $\gamma \in \mathcal{Z}$ **do**
    $\theta_\gamma \leftarrow \mathbf{A}_\gamma^{-1}\mathbf{b}_\gamma$
    $f_{i,\gamma} \leftarrow \mathbf{w}_{i,\gamma}^T\theta_\gamma + \alpha\sqrt{\mathbf{w}_{i,\gamma}^T\mathbf{A}_\gamma^{-1}\mathbf{w}_{i,\gamma}}$
  Select arm $\Phi^* = \underset{\gamma\in\mathcal{Z}}{\text{argmax}}\, f_{i,\gamma}$ and observe reward r_{i,Φ^*};
  $\mathbf{A}_{\Phi^*} \leftarrow \mathbf{A}_{\Phi^*} + \mathbf{w}_{i,\Phi^*}\mathbf{w}_{i,\Phi^*}^T$
  $\mathbf{b}_{\Phi^*} \leftarrow \mathbf{b}_{\Phi^*} + r_{i,\Phi^*}\mathbf{w}_{i,\Phi^*}$

3.2 Thompson Sampling Semi-Bandits

In the architecture, loss is directly related to rewards of all contextual bandits, resulting in the obstacles in quantifying combinatorial head contribution due to the more significant parts that dynamic layers play. Besides, it is much tougher to measure combinatorial dynamics by modeling continuous value compared with the concrete number selections of numerical dynamics. To address the issues, our work simplifies the observations of superarm as binary values, whose feedback is polarily classified as one otherwise zero. To this end, our work are able to detect the most efficient head combinations by dynamically clustering all heads into two groups.

Let us assume that reward $r_i \in 0,1$ is Bernoulli distributed with $P_r(r_i = 1|\mathbf{w}_{i,\gamma})$ (Wang et al., 2017). Let us initialize the mean vector as $\mathbf{g}_{i,\gamma} = \mathbf{I}^{2d\times 1}$ and inverse covariance as $\mathbf{s}_\gamma = \mathbf{0}^{2d\times 2d}$. In order to learn the likelihood probability of reward 1, the learnable weight vector $\mathbf{p}_{i,\gamma} \in R^{2d}$ approximates $E_{i,\gamma} = P_r(r_i = 1|\mathbf{w}_{i,\gamma})$ as

$$\mathbf{p}_{i,\gamma} = \mathbf{N}(\mathbf{g}_\gamma, \mathbf{s}_\gamma{}^{-1}), \quad (3)$$

$$\mathbf{E}_{i,\gamma} = \sigma(p^{T}{}_{i,\gamma}\mathbf{w}_{i,\gamma}), \quad (4)$$

where σ is the sigmoid function and N is the normal distribution. The learner chooses K actions out of the whole set Z, thus the optimal combinatorial subset is selected according to the K highest $\mathbf{E}_{i,\gamma}$. We denote the optimal subset as

$$\Phi^* : \{\gamma_1, \gamma_2, \ldots, \gamma_K\} \subset \mathbf{Z}. \quad (5)$$

After the TSB is executed, we receive a binary reward ri as the e feedback of Φ^* to refresh N. The estimation on refreshed $\hat{g}_\gamma$ is to find the maximizer (Bishop, 2006):

$$\frac{1}{2}\sum_{j=1}^{2d}\mathbf{s}_\gamma(\mathbf{p}_\gamma - \mathbf{g}_\gamma)^2 + \sum_{i=1}^{n}\log(\sigma(r_i\mathbf{p}^T{}_\gamma\,\mathbf{w}_{i,\gamma}))), \quad (6)$$

where j is the index of the feature dimension of the vector, λ is the regularization parameter. Then we update $\mathbf{s}_\gamma$

$$\mathbf{s}_\gamma = \mathbf{s}_\gamma + \sum_{i=1}^{n}\sigma(\mathbf{p}^T{}_\gamma\,\mathbf{w}_{i,\gamma})(1 - \sigma(\mathbf{p}^T{}_\gamma\,\mathbf{w}_{i,\gamma}))\mathbf{w}^2{}_{ij,\gamma}. \quad (7)$$

4. PROPOSED METHODOLOGY

In this section, we will discuss our sample-based search on transformer attention space. Our model begins by recalling the multi-head attention and head masking mechanism. Then, our paper introduces the definitions of states, actions for deciding heads and layers. Lastly, our paper demonstrates how to formulate rewards to update all contextual bandits based on the searching routine.

Our core objective is to flexibly fabricate multiple bandits into the transformer framework to search for optimal network update routine given each input. Our work design two search modes to demonstrate DHT training, constructing UCB as numerical dynamics and TSB as combinatorial dynamics for selecting the number of heads (layers) and head combinations, respectively.

4.1 Multi-Head Attention and Pruning

Given the input feature vector $\mathbf{x}_l \in R^d$ at l-th layer of an input sample $\mathbf{x} \in R^d$, the pruned multi-attention layer function $f_l(\mathbf{x}_l)$ can be formulated as follows [3,46].

$$f_l(\mathbf{x}_l) = \sum_{h=1}^{N}\xi_h \mathrm{Att}_{W_{k,h},W_{ql,h},W_{vl,h},W_{ol,h}}(\mathbf{x}_l), \quad (8)$$

where Att is the single-head attention parameterized by $W_{k,h}$, $W_{ql,h}$, $W_{vl,h}$, $W_{ol,h} \in R^{d\times d}$, N_h is the number of full heads, and ξh is the masking variable with values in { 0, 1} and each value corresponds to heads in relative

positions. Simplifying the notation of the single attention for a head h in Equation (8) as Att_h, our model define the combinatorial heads as $\mathbf{\Pi}l = \{\xi_1\text{Att}_1, ..., \xi_{\text{Nh}}\text{Att}_{\text{Nh}}\}$. If all ξhs are equal to 1, the formula corresponds to the multi-attention layer in a vanilla Transformer model. If some ξh have values of 0, the corresponding heads are pruned in the layer. The preserved number of heads is hence

Algorithm 2: Architecture Space Search

1 **for** *all* **x do**
2 **x** passes the first b layer weights at last round and stops at S_1;
3 **if** *Mode = Tree Search* **then**
4 Run UCB_L and obtain $L \leftarrow \Phi^*_L \in Z_L$;
5 **else**
6 Run UCB_{cp} and obtain $(L, H) \leftarrow \Phi^*_{cp} \in Z_{cp}$;
7 **x** repasses the first b layer weights and stops at $S_{2,0}$;
8 **if** $L>0$ **then**
9 **while** $l \leq L$ **do**
10 **if** *Mode = Tree Search* **then**
11 Run UCB_H to obtain $H_l \leftarrow \Phi^*_{H,l} \in Z_H$;
12 Run TSB to obtain the head combination $\mathbf{\Pi}_l \leftarrow \Phi^*_{ts,l}$ with H_l heads;
13 $l \leftarrow l + c$
14 Sample(s) proceed(s) c layer(s) with H_l heads and stops at $S_{2,l}$;
15 **x** finishes $(b + L)$ layer(s) with adaptive heads and obtain the loss of **x**;
16 Receive rewards: $r_{\Phi^*_L}, r_{\Phi^*_{H,l}}$ ($r_{\Phi^*_{cp}}$) and $r_{\Phi^*_{ts,l}}$ as Equation (10) - (15);
17 Update all contextual bandits;

Algorithm 3: Queuing Strategy

Input: Data sample $\mathbf{x}_{t,i} \in \mathcal{X}_t$ with corresponding layer number L_n
1 **for** *all* $\mathbf{x}_{t,i}$ *and* L_n **do**
2 Allocate $\mathbf{x}_{i,t}$ to join $\mathbf{Q}_{L_n}$ at S_1;
3 **if** $len(\mathbf{Q}_{L_n}) = q$ **then**
4 All samples in $\mathbf{Q}_{L_n}$ are released and proceed as line 7 - 16 in Algorithm 2;
5 $len(\mathbf{Q}_{L_n}) \leftarrow 0$.

4.2 Architecture Space Search

Let the maximum number of layers a Transformer can have be N_L, sample **x** only needs to go through $L \leq N_L$ layers as search limit during training or inference to obtain good performance.

To balance the trade-off between searching comprehensiveness and computational efficiency, we present two searching modes to enhance searching flexibility: tree search and integrated search, with the former focusing on comprehensiveness and the latter efficiency. In the case of tree search, there are two UCBs: UCB_L and UCB_H to make decisions on L and H_l, respectively. UCB_L is executed once to determine L, namely the number of layers a sample **x** needs to go through. UCB_H and TSB are utilized to jointly determine the number of heads to preserve and which heads to preserve for each layer, respectively. To speed up the training, our work employs UCB_H and TSB not for every single layer l, but rather for a group of c adjacent layers, to determine the pruning information for all c layers at once. In the case of integrated search, instead of determining the number of layers L and the number of heads at each layer H_l separately, our work uses one complex UCB_{cp} to determine L and H at once, i.e. the number of heads to keep at each layer is the same. However, our work still applies TSB on every c adjacent layer to determine the combination of heads $_l$ to keep.

The optimal arms are Φ^*_L, $\Phi^*_{H,l}$ or Φ^*_{cp}, and the optimal superheads are $\Phi^*_{ts,l}$ at l-th depth. To obtain the arm features, our model pass all samples through all layers of the full model once, without back propagation. For each option of layer numbers in our DHT model (i.e. $L = 3$, $L = 6$, etc.), our model takes all sample outputs of the model (feature representation matrices) and computes an average as the arm feature for UCB_L corresponding to the layer depth. e.g., the arm feature of $L = 3$ is the average of all samples' output matrices at the end of 3rd layer, the arm feature of $L = 6$ is the average of all samples' output matrices at the end of 6th layer. Similarly, to obtain UCB_H, each sample is randomly and evenly assigned a head number given each layer. Our model averages all sample feature representation matrices as the arm feature corresponding to the same head number. If the searching mode is complex, the arm feature of UCB_{cp} is the average of all samples' feature vector at both corresponding same layer depth and head number, such as the arm feature of $L = 3$, $H = 8$ is the average of all feature representation matrices at 3rd layer with 8 preserved heads. In terms of the arm feature of TSB, our model collects all feature representation matrices at all layers with all kinds of head numbers, and split each vector into N_H submatrices along the embedding dimension space. Each averaged sub-matrix corresponds to a specific head, formulating the arm feature of the corresponding TSB arm feature. Thus there are N_H TSB arms in total.

In the following, our work illustrates both searching modes using an example sample **x**. Because our model needs some contextual information of **x** during each training epoch, the first b layers of the model are kept unpruned. All remaining layers are dynamic and c is a hyperparameter serving as the number of adjacent layers UCB_H and TSB jointly operate on to determine the number of heads and the combination of heads to keep. $\mathbf{w}_L$, $\mathbf{w}_{H,l}$ are the aggregated vectors at l-th layer for UCB_L and UCB_H.

4.2.1 Tree Search

Step 1 $l = b$
x initially passes through the first b layers to reach state S_1. Our work combines $\mathbf{x}_l$ with the arm feature vector to formulate a set of aggregated vector $\mathbf{w}_L$. The weights of b layers are inherited from t-1. UCB_L selects Φ^*_L to find L, the number of layers **x** needs to pass through.

Step 2 $l = b$
x repasses through the first b layers to reach $S_{2,0}$, during which layer weights are updated through back-propagation. Our model continues to execute UCB_H to obtain all H_l for the next group of c layer(s). Similarly, our model constructs the aggregated vector $\mathbf{w}_{H,l} = [\mathbf{x}_l ; Z_{H,l}; \mathbf{e}_l]$, where $\mathbf{e}_l$ is a column one-hot vector

to mark the layer depth. According to $\Phi^*_{H,l}$, TSB is employed to select $\Phi^*_{ts,l}$ to obtain $\mathbf{\Pi}_l$. Note that for all upcoming c layer(s), the heads to be pruned are in the same relative positions.

Step 3 $l = b + oc$
Our model increments o by one, where o is the number of times UCB_H and TSB have been executed. If $l < b + L$, go back to step 2 and repeat UCB_H and TSB; otherwise, go to step 4.

Step 4 $l = b + L$
Our model observe the reward r_{Φ^*L}, $r_{\Phi^*H,l}$ and $r_{\Phi^*ts,l}$ and begins the back-propagation.

4.2.2 Integrated Search

Step 1 and 2 $l = b$
Similar to step 1 and 2 in the tree search, our model first utilizes UCB_{cp} to obtain both L and H for $\mathbf{x}$ at S_1. Then, $\mathbf{x}$ proceeds through the first b layer(s) again and stop at $S_{2,0}$.

Step 3 $l = b + oc$
Our model increments by one and, if $l < b + L$, go back to step 2 and run the TSB and obtain the head combinations $\mathbf{\Pi}_l$ with H heads; otherwise, our model moves forward to step 4.

Step 4 $l = b + L$
Our model observe the reward $r_{\Phi^*_{cp}}$ and $r_{\Phi^*_{ts,l}}$ and begins the back-propagation.

4.3 Reward Formulation

According to the rule of Markov Decision Process, the current state depends on the previous one. Therefore, our model formulates rewards through comparing loss and the number of heads and layers between the current batch samples and the past batch samples together to maximize the cumulative training rewards. Given a sequential input batch samples $\mathbf{x}=\{\mathbf{x}_1, \ldots, \mathbf{x}_i\}$ at time stamp t, $L_{t,i}$ and $H_{t,i,l}$, the number of layers and heads selected for $\mathbf{x}_{t,i}$, serve as the search limit, and $\delta_{L,t,i}$, defined below, is the product of loss and $L_{t,i}$.

$$\delta_{L,t,i} = loss(\mathbf{x}_{t,i}) \cdot L_{t,i}. \quad (9)$$

The reward $r_{\Phi^*L,t,i}$ at timestamp t for i-th sample is

$$r_{\Phi^*L,t,i} = \alpha \cdot \frac{\sum_{j=1}^{bs} (\delta 1,t-1,j)/bs}{\delta t,i}, \quad (10)$$

where α is the positive hyper-parameter. A smaller $\delta_{L,t,i}$ in Equation (10) denominator represents fewer losses (better training results) and fewer layers (fewer costs) for the sample at the ongoing round in relation to averaged gains during the last round, so the reward will be higher to encourage this trend. Similarly, with β_1 and βcp as the hyper-parameters for head tuning, $\delta_{H,t,i,l}$ and $\delta_{cp,t,i,l}$ as the products of loss, number of layers and heads at the l-th layer for UCB_H and UCB_{cp}, defined below

$$\delta_{H,t,i,l} = \text{loss}(\mathbf{x}_{t,i}) \cdot L_{t,i} \cdot H_{t,i,l},,, \quad (11)$$
$$\delta_{cp,t,i,l} = \text{loss}(\mathbf{x}_{t,i}) \cdot L_{t,i} \cdot H_{t,i,l},,, \quad (12)$$

rewards for UCB_H and UCB_{cp} are

$$r_{\Phi*} H,t,i,l = \beta_1 \cdot \frac{\sum_{j=1}^{bs} (\delta 2,t-1,j)/bs}{\delta 2,t,i,l}, \quad (13)$$

$$r_{\Phi*} cp,t,i,l = \beta_1 \cdot \frac{\sum_{j=1}^{bs} (\delta cp,t-1,j)/bs}{\delta cp,t,i,l}, \quad (14)$$

Inspired by a work that illustrates some positional heads steadily contribute significantly and others work incrementally or negatively (Voita et al., 2019), we simplify our observations of combinatorial heads Πt,i,l as binary values, where 1 is more effective and 0 is less effective when compared with superheads in the previous batch Πt−1,i,l.

$$r_{\Phi*} ts,i,l = 0, \text{ if } r_{\Phi*} H,t,i\ (r_{\Phi*} cp,t,i,l) > 1,$$
$$r_{\Phi*} ts,i,l = 1, \text{ if } r_{\Phi*} H,t,i\ (r_{\Phi*} cp,t,i,l) \leq 1. \quad (15)$$

5. Implementation

During training, our model first constructed arm feature vectors for all contextual bandits. Then, our model trains all samples dynamically by utilizing sample-dependent layer and head combination information provided by UCB_L, UCB_H and TSB, as described in Section 4. Because each sample corresponds to a different number of layers, as is determined by UCB_L, our model cannot directly group samples into batches since our model will not have known the appropriate model with the right L layers for those samples. Therefore, our model implement a queuing strategy that categorizes each sample into a particular queue based on the optimal $L = L^*$, determined for it enabling the parallel execution of UCBs and TSB.

Let $\{Q=Q_{L1}, \ldots, Q_{Ln}\}$ be a set of queues corresponding to a set of layer numbers $\{L_1, \ldots, L_n\}$, where each queue has a size of q. After the execution of UCB_L or UCB_{cp}, $\mathbf{x}_{t,i}$ with L_n is allocated to the corresponding queue Q_Ln. When the number of samples inside Q_Ln reaches q, all are required to form a batch. Otherwise, samples will temporarily stay in the queue and wait for more corresponding samples to be added. There is no training or inference until one queue is full at S_1.

It is probable that the samples in one queue come from different time rounds, so our model just use the historical weights of the first b-th layer to obtain S1 without updating any neutral networks until the training batch is created. $S_{2,0}$ is reached upon all samples having passed the first b-th layers. In this way, our model stabilizes the accuracy of gradient。

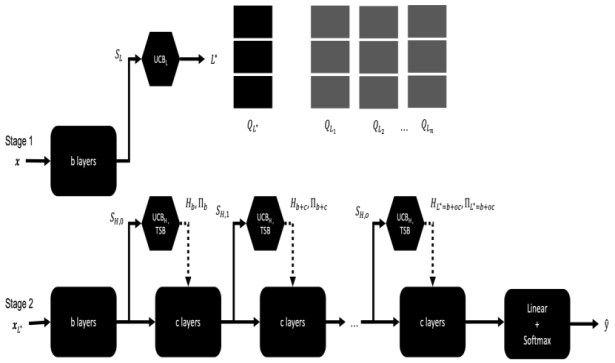

Figure 1. Illustration of DHT model training. Here, a solid arrow means the data is pass to model layers and a a dotted arrow means the information determined by UCBs and TSBs at a particular state S is used to formulate the upcoming c layers in the dynamic model. Our model first determine the number of layers needed for a particular sample x, L^* in our example. Then, our model put x into a queue corresponding to the required number of layers L^*. Once a queue for L^* is filled up, our model compile all samples in the queue to form a batch $\mathbf{x}_{L*}$. Afterwards, our model pass $\mathbf{x}L*$ through the first b layers in order to obtain such information as the number of heads and head combinations for the upcoming c layers. Our model repeats the process o time such that $L = b + oc$. Lastly, our model updates our model with rewards computed based on y hat.

descent and ensure the training effects. Our queuing strategy is summarized in Algorithm 3.

6. EXPERIMENTS

In this section, our work first describes our experiment configurations. Then, the section describes the baseline models to be compared with and the dataset on which our work runs the experiments, and analyzes the experiment results.

6.1 Configurations

Our work experimented with four configurations under the standard 12-layer and 12- head framework. The embedding size is 768 and sequence length varies among datasets. The hyperparameters b and c are 3. Along with the preset configurations for L, this guarantees that L, b is divisible by o, the number of times UCB_H and TSB get executed.

Tree-search DHT (T-DHT): Following the tree search mode, the options for the number of T-DHT layer (L) are 3,6,9,12, and and the options for number of heads (H) at each layer are 8,10,12, each corresponding to 70, 28, 1 type(s) of head combination(s).

Specialized DHT (S-DHT): Following the integrated search mode, this configuration only applies specialized dynamics to DHT to explore the least contextual bandits execution. The available options of UCB_{cp} are 3L12H, 6L12H, 9L12H, 12L8H, 12L10H, 12L12H. Specifically, 3L12H means the model has three layers and each layer has twelve heads.

Full DHT (F-DHT): Following the integrated search mode, this configuration concentrates on full dynamics for DHT. The available options of UCB_{cp} are 3L12H, 6L8H, 6L10H, 6L12H, 9L8H, 9L10H, 9L12H, 12L8H, 12L10H, 12L12H.

Partial-frozen DHT (P-DHT): First, model training follows the configuration of Full DHT (F-DHT) for two epochs. Afterwards, our work train all but the last two layers by freezing their weights. The available options of UCB_{cp} are 1L8H+2L12H, 1L10H+2L12H, 1L12H+2L12H, 4L8H+2L12H, 4L10H+2L12H, 4L12H+2L12H, 7L6H+2L12H, 7L9H+2L12H, 7L12H+2L12H, 10L8H+2L12H, 10L10H+2L12H, 10L12H+2L12H. Specifically, 1L8H+2L12H means there are three layers in total, where the first layer has eight heads and the last two layers have twelve heads each.

6.2 BASELINES, DATASETS AND ANALYSIS

We use four text classification datasets (Zhang et al., 2016) to evaluate the DHT configurations: Dbpedia Dataset (Dbpedia), Ag News Dataset (Ag. News) , Yelp Review Polarity Dataset (Yelp.P) and Yelp Review Full Dataset (Yelp.F). Floating-point operation (FLOP) is a measure of the computational complexity of models. We quantify our computational efficiency using a FLOP ratio regarding the full vanilla BERT with 12 layers and 12 heads as the baseline. That is, if our configuration is twice as efficient as the vanilla BERT model, then our FLOP ratio is 0.50x, etc.. In addition, we record F1-score to characterize the accuracy of classification tasks. We compare DHT from scratch against three baselines, including sample-based lightening, layer only distillation and the vanilla BERT model. For the FLOP ratio comparison, DHT is compared with baseline 1 (BL1) for training and with all baselines for inference. Baseline 2 and 3 are trained with full layers and heads. All FLOP ratios are estimated based on the layer/head number selection in comparison with a model with full layers and full heads. BL1: Full Vanilla BERT (12-VaBERT) with 12 layers and 12 heads. We define our benchmark FLOP ratio (1.00x) in training and inference based on its FLOP count. BL2: DistilBERT (Sanh et al., 2020) released by Huggingface with 1, 3, 6 distilled layers, where each configuration of distilled layers corresponds to FLOP ratio of 0.08x, 0.25x, 0.50x regarding 12- VaBERT. This is the most classical method for reducing BERT inference complexity. We denote them as 1, 3, 6-DisBERT, respectively. BL3: Adaptive sample-based FastBERT using knowledge distillation. The decision on depth selection relies on the preset inference speedup: 0.1x, 0.5x, and 0.8x (approximately FLOP ratios of 0.08x, 0.25x, 0.50x regarding 12-VaBERT, depending on different datasets). We denote them as 1,3,6-FastBERT, respectively. From

Table 1, we can see that most DHT training costs are lower than 0.5 in relative to the vanilla BERT model. In particular, the cost of S-DHT is even lower than 0.3 for Yelp. P and Yelp. F. That means, in theory, our DHT models can be trained more efficiently. From Table 2, we can see that DHT models also have competitive accuracy with significant complexity mitigation. Specifically, in comparison with baseline 2, our DHT models outperform the uniform-level knowledge distillation in both model complexity and inference accuracy. In comparison with baseline 3, we have competitive inference performance in terms of more economic training costs. That is, even though our inference costs are higher than those of FastBERT, our accuracy does not decrease as dramatically. Integrating both inference and training costs, DHT are apparently more advantageous than DisBERT. Furthermore, the mechanism of DHT is different from that of DisBERT and FastBERT, where the level of computational complexity is reduced in the beginning. DHT takes care of training effects and costs simultaneously and dynamically, so the accuracy loss is minimal even with tremendous speedup, such as 0.26x speedup for both training and inference of S-DHT for Yelp. P but accuracy loss is only 0.6% in relation to vanilla BERT, 0.29x speedup for training and 0.26x for inference of S-DHT for Yelp. F but only 4.1% accuracy loss, according to Table 2.

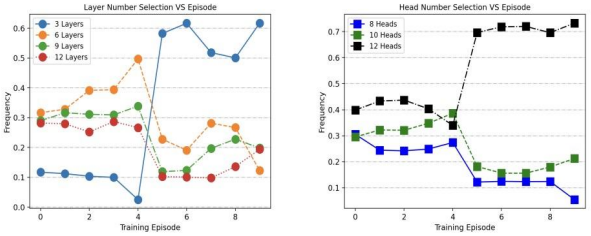

(a) P-DHT Dynamics for **Ag. News**: Layer number, head number selection

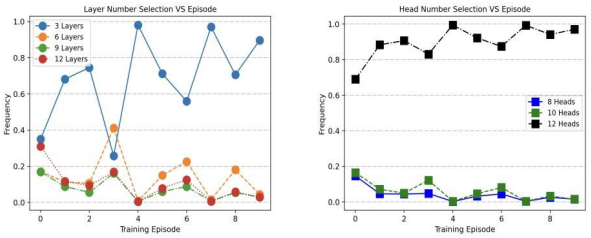

(b) S-DHT Dynamics for **Ag. News**: Layer number, head number selection

Figure 2. We illustrate here the trends of layer number and head number throughout training. We observe that the selection of 3-layer configuration with 12 heads on each layer becomes dominant as training progresses forward. This indicates that our DHT models indeed adapt themselves to reduce computational cost for training and inference.

6.3 DIVE INTO THE DYNAMICS: LAYER, HEAD AND TRAINING STABILITY

From Figure 2a, we can see that the 3-layer option is selected less frequently in the beginning and more frequently after 5 episodes. In contrast, other layer options demonstrate downtrends as training progresses forward. This indicates that, throughout time, the less complex option regarding the number of layers is chosen by the trained UCBL model, so training costs are gradually decreasing. With respect to head selection, the 12-head option is dominant towards the end of the training. From Figure 3, we can see that although the layer routine is adaptive across the training, the loss maintains the downtrend and then converges smoothly. It proves that dynamic training is effective for mitigating complexity without hurting training stability.

7 CONCLUSIONS

In this work, we propose to search optimal layers and heads hierarchically via contextual bandits. Contextual bandits are deployed at low costs and successfully reduce the computational complexity for both model training and inference while maintaining the model performance. The objective of DHT is to maintain the model performance with self-adaptive training and inference mechanism, which takes care of both the goal of automatic machine learning (AutoML) and model compression. We investigate many aspects in the paper such as dynamic weights training, weight pruning and sample-based training. Different from traditional network compression methods, our approach is customized by layerwise and headwise dynamics with more sample-oriented flexibility, which means less inference accuracy loss. On the other hand, the down-to-top order optimization is much more efficient than top-to-down streaming in NAS. In the future, we hope to extend this methodology into more deep learning frameworks.

Table 1: Training Comparisons: Inference F1 scores (F1) and ratios of the FLOP count of our four DHT configurations to that of BL1.

Model & Datasets	F1 (Ag)	FLOP (Ag)	F1 (DB)	FLOP (DB)	F1 (YP)	FLOP (YP)	F1 (YF)	FLOP (YF)
BL1	0.944	1.00	0.993	1.00	0.960	1.00	0.659	1.00
T-DHT	0.945	0.42	0.932	0.43	0.958	0.47	0.635	0.45
P-DHT	0.935	0.59	0.993	0.41	0.955	0.44	0.634	0.58
S-DHT	0.941	0.38	0.994	0.39	0.956	0.26	0.632	0.29
F-DHT	0.943	0.59	0.993	0.58	0.957	0.29	0.639	0.43

Table 2: Inference Comparisons: F1 scores (F1.) and ratios of the FLOP count of our four DHT configurations to that of the BL1, BL2 and BL3.

Model & Datasets	F1 (Ag)	FLOP (Ag)	F1 (DB)	FLOP (DB)	F1 (YP)	FLOP (YP)	F1 (YF)	FLOP (YF)
BL1	0.944	1.00	0.993	1.00	0.960	1.00	0.659	1.00
BL2 - 6 layer	0.946	0.50	0.991	0.50	0.953	0.50	0.642	0.50
BL2 - 3 layer	0.939	0.25	0.990	0.25	0.932	0.25	0.635	0.25
BL2 - 1 layer	0.928	0.08	0.989	0.08	0.916	0.08	0.585	0.08
BL3 - 6 layer	0.943	0.28	0.992	0.10	0.959	0.31	0.659	0.95
BL3 - 3 layer	0.931	0.010	0.990	0.09	0.960	0.16	0.659	0.95
BL3 - 1 layer	0.925	0.08	0.990	0.09	0.960	0.08	0.647	0.46
T-DHT	0.945	0.81	0.992	0.76	0.958	0.83	0.635	0.87
P-DHT	0.935	0.39	0.993	0.41	0.965	0.28	0.634	0.35
S-DHT	0.941	0.37	0.994	0.44	0.956	0.26	0.632	0.26
F-DHT	0.943	0.35	0.995	0.29	0.957	0.31	0.639	0.29

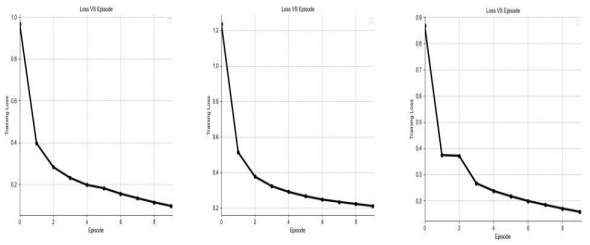

Figure 3. Loss Trends: P-DHT for Ag. News, S-DHT for Ag. News and F-DHT for Yelp. P.

A APPENDIX A.1 SAMPLING METHODS

In natural language processing, the input has three dimensions, i.e. batch size bs, sequence length sl and embedding size emb, our sampling is based on one instance (bs = 1). Because each sample corresponds to sl × emb features, keeping all features can be very memory expensive. Therefore, for all contextual bandits, we use mean pooling as the sampling method to generate context or arm vectors in order to reduce the memory footprint.

In terms of either sl or emb, we perform mean pooling iteratively and interchangeably. The elements in one dimension is sequentially and evenly split into: 1, 2, 4, 6, 8, ..., 2n parts. Depending on the choice of n and initial value m for i, we have $\sum_{i=m}^{n} = 2^i$ sampled features for this dimension. For example, iif we are sampling for the sequence length (sl) dimension and n = 2 and m = 0, the new feature is composed of seven sampled vectors: mean($sl_{1,1}$), mean($sl_{2,1}$), mean($sl_{2,2}$), mean($sl_{4,1}$), mean($sl_{4,2}$), mean($sl_{4,3}$), mean($sl_{4,4}$). There are two values in each subscript. The first one indicates for the selected dimension (i.e. sl) how many parts the original input is split, and the second one indicates for which segment of the split input we compute the mean value for.

In our experiment, we first sample from sl and then sample from emb. Specifically, for UCBL and UCBcp we first sample (1 + 2) = 3 sl features and 4 + 8 + 16 = 26 emb features; for UCB_H we first sample (1 + 2) = 3 sl features and 2 + 4 + 8 = 14 emb features; for TSB we first sample (1) = 1 sl features and 4 + 8 = 12 emb features. As a result, the dimension of the sampled UCB_L and UCB_{cp} context vectors is (1, 3 × 36), the dimension of the sampled UCB_H context vector is (1, 3 × 14) and the dimension of the sampled TSB context vector is (1, 1 × 12).

A.2 NORMALIZATION METHODS

In this end, the context vectors are sampled from instance representations in time step, so they appear in time series and rolling (running) normalization is better for fitting linear distributions of users. The normalization algorithm is introduced by (Ogasawara et al., 2010).

A.3 DATASETS

Ag. News contains 120,000 training datasets and 7,600 testing datasets with four classes. We set 128 as sequence length.

Dbpedia contains 560,000 training datasets and 70,000 testing datasets with fourteen classes. We set 128 as sequence length.

Yelp. P contains 560,000 training datasets and 38,000 testing datasets with two classes. We set 300 as sequence length.

Yelp. F contains 650,000 training datasets and 50,000 testing datasets with five classes. We set 300 as sequence length.

A.4 CONTEXTUAL BANDITS SETTINGS

We set the size of the training sample vector of UCBL (UCB_{cp}), UCB_H and TSB as 168, 87, 13 respectively. The learning rate is adaptive to the types of datasets, we normally run the whole training process for 3 to 6 epochs. Each experiment is conducted on NVIDIA GTX 1080, GTX 2080, Tesla V100 16G GPU separately.

A.5 SUPPLEMENTARY RESULTS AND ANALYSIS

We complement analysis on different configurations besides Section 6.3. S-IDHT in Figure 7 aligns with the trends with Figure 3 in content. From Figure 4 concerning F-IDHT, 3 layers is also selected mostly but the frequency is stable, 6 layers is secondary and stable as well. In terms of Figure 6 concerning T-DHT, 12 layers are the least one firstly and gradually dominant (≈ 1.0) after 4 episodes. With regards to head selection, 12 heads presents downtrend and 8 heads and 12 heads are in uptrend for F-IDHT. 8 heads and 12 heads are preferable by T-DHT after 3 episodes. For TSB superhead selection, as long as the incomplete multi-heads attentions are chosen, two figures align with previous analysis that some heads are less contributive to model performances and maintain their roles across the training (No. 10, No. 11 in Figure 5 and 7, No.1, No.3, No.6 in 14 Figure 6). From loss trends, the tendencies for two configurations are the same that training stability is not negatively affected by dynamic layer routines.

References:

[1] https://en.wikipedia.org/wiki/O%27Hare_International_Airport
[2] Sundarapandian, V. (2009). "7. Queueing Theory". Probability, Statistics and Queueing Theory. PHI Learning. ISBN 978-81-203-3844-9.
[3] Aishwarya Bhandare, Vamsi Sripathi, Deepthi Karkada, Vivek Menon, Sun Choi, Kushal Datta, and Vikram Saletore. Efficient 8-bit quantization of transformer neural machine language translation model, 2019. Christopher M. Bishop. Pattern Recognition and Machine Learning (Information Science and Statistics). Springer-Verlag, Berlin, Heidelberg, 2006. ISBN 0387310738.
[4] Antoine Bosselut, Hannah Rashkin, Maarten Sap, Chaitanya Malaviya, Asli Celikyilmaz, and Yejin Choi. Comet: Commonsense transformers for automatic knowledge graph construction, 2019.
[5] Tom B. Brown, Benjamin Mann, Nick Ryder, Melanie Subbiah, Jared Kaplan, Prafulla Dhariwal, Arvind Neelakantan, Pranav Shyam, Girish Sastry, Amanda Askell, Sandhini Agarwal, Ariel Herbert-Voss, Gretchen Krueger, Tom Henighan, Rewon Child, Aditya Ramesh, Daniel M. Ziegler, Jeffrey Wu, Clemens Winter, Christopher Hesse, Mark Chen, Eric Sigler, Mateusz Litwin, Scott Gray, Benjamin Chess, Jack Clark, Christopher Berner, Sam McCandlish, Alec Radford, Ilya Sutskever, and Dario Amodei. Language models are few-shot learners, 2020. Haw-Shiuan Chang, Erik Learned-Miller, and Andrew McCallum. Active bias: Training more accurate neural networks by emphasizing high variance samples. Advances in Neural Information Processing Systems, 30:1002–1012, 2017.
[6] Insoo Chung, Byeongwook Kim, Yoonjung Choi, Se Jung Kwon, Yongkweon Jeon, Baeseong Park, Sangha Kim, and Dongsoo Lee. Extremely low bit transformer quantization for on-device neural machine translation, 2020.
[7] Jacob Devlin, Ming-Wei Chang, Kenton Lee, and Kristina Toutanova. Bert: Pre-training of deep bidirectional transformers for language understanding, 2019.
[8] Maha Elbayad, Jiatao Gu, Edouard Grave, and Michael Auli. Depth-adaptive transformer, 2020.
[9] Song Han, Jeff Pool, John Tran, and William J. Dally. Learning both weights and connections for efficient neural networks, 2015. Song Han, Huizi Mao, and William J. Dally. Deep compression: Compressing deep neural networks with pruning, trained quantization and huffman coding, 2016.
[10] Geoffrey Hinton, Oriol Vinyals, and Jeff Dean. Distilling the knowledge in a neural network, 2015. Jon Hoffman. Cramnet: Layer-wise deep neural network compression with knowledge transfer from a teacher network, 2019.
[11] Lu Hou, Zhiqi Huang, Lifeng Shang, Xin Jiang, Xiao Chen, and Qun Liu. Dynabert: Dynamic bert with

adaptive width and depth, 2020. Xiaoqi Jiao, Yichun Yin, Lifeng Shang, Xin Jiang, Xiao Chen, Linlin Li, Fang Wang, and Qun Liu. Tinybert: Distilling bert for natural language understanding, 2020.

[12] Jae-young Jo and Sung-Hyon Myaeng. Roles and utilization of attention heads in transformer-based neural language models. In Proceedings of the 58th Annual Meeting of the Association for Computational Linguistics, pp. 3404–3417, Online, July 2020. Association for Computational Linguistics. doi: 10.18653/v1/2020.acl-main.311. URL https://www.aclweb.org/anthology/2020.acl-main.311.

[13] Hyeji Kim, Muhammad Umar Karim Khan, and Chong-Min Kyung. Efficient neural network compression. In Proceedings of the IEEE/CVF Conference on Computer Vision and Pattern Recognition (CVPR), June 2019. Shakti Kumar, Jerrod Parker, and Panteha Naderian. Adaptive transformers in rl, 2020. Eunho Lee and Youngbae Hwang. Layer-wise network compression using gaussian mixture model. Electronics, 10(1), 2021. ISSN 2079-9292. doi: 10.3390/electronics10010072. URL https://www.mdpi.com/2079-9292/10/1/72.

[14] Lihong Li, Wei Chu, John Langford, and Robert E. Schapire. A contextual-bandit approach to personalized news article recommendation. Proceedings of the 19th international conference on World wide web - WWW '10, 2010. doi: 10.1145/1772690.1772758. URL http://dx.doi.org/10.1145/1772690.1772758.

[15] Zuchao Li, Zhuosheng Zhang, Hai Zhao, Rui Wang, Kehai Chen, Masao Utiyama, and Eiichiro Sumita. Text compression-aided transformer encoding. IEEE Transactions on Pattern Analysis and Machine Intelligence, pp. 1–1, 2021. doi: 10.1109/TPAMI.2021.3058341.

[16] Weijie Liu, Peng Zhou, Zhe Zhao, Zhiruo Wang, Haotang Deng, and Qi Ju. Fastbert: a self-distilling bert with adaptive inference time, 2020.

[17] Andre Teixeira Lopes, Edilson De Aguiar, Alberto F De Souza, and Thiago Oliveira-Santos. Facial ´ expression recognition with convolutional neural networks: coping with few data and the training sample order. Pattern recognition, 61:610–628, 2017.

[18] Jian-Hao Luo, Jianxin Wu, and Weiyao Lin. Thinet: A filter level pruning method for deep neural network compression. In Proceedings of the IEEE International Conference on Computer Vision (ICCV), Oct 2017.

[19] R.A. McCallum. Hidden state and reinforcement learning with instance-based state identification. IEEE Transactions on Systems, Man, and Cybernetics, Part B (Cybernetics), 26(3):464–473, 1996. doi: 10.1109/3477.499796.

[20] Paul Michel, Omer Levy, and Graham Neubig. Are sixteen heads really better than one? In H. Wallach, H. Larochelle, A. Beygelzimer, F. d'Alche-´ Buc, E. Fox, and R. Garnett (eds.), Advances in Neural Information Processing Systems, volume 32, pp. 14014–14024. Curran Associates, Inc., 2019a. URL https://proceedings.neurips.cc/paper/2019/file/2c601ad9d2ff9bc8b282670cdd54f69f-Pap

[21] Paul Michel, Omer Levy, and Graham Neubig. Are sixteen heads really better than one?, 2019b.

[22] Pavlo Molchanov, Arun Mallya, Stephen Tyree, Iuri Frosio, and Jan Kautz. Importance estimation for neural network pruning, 2019. James O' Neill. An overview of neural network compression, 2020.

[23] Eduardo Ogasawara, Leonardo C. Martinez, Daniel de Oliveira, Geraldo Zimbrao, Gisele L. Pappa, ˜ and Marta Mattoso. Adaptive normalization: A novel data normalization approach for nonstationary time series. In The 2010 International Joint Conference on Neural Networks (IJCNN), pp. 1–8, 2010. doi: 10.1109/IJCNN.2010.5596746.

[24] Victor Sanh, Lysandre Debut, Julien Chaumond, and Thomas Wolf. Distilbert, a distilled version of bert: smaller, faster, cheaper and lighter, 2020.

[25] Zein Shaheen, Gerhard Wohlgenannt, and Erwin Filtz. Large scale legal text classification using transformer models, 2020.

[26] Sainbayar Sukhbaatar, Edouard Grave, Piotr Bojanowski, and Armand Joulin. Adaptive attention span in transformers, 2019.

[27] Meng, Fanfei, and Yuxin Wang. "Transformers: Statistical interpretation, architectures and applications." (2023).

[28] Fanfei Meng, Branden Ghena. (2023) Research on Text Recognition Methods Based on Artificial In-telligence and Machine Learning. Advances in Computer and Communication, 4(5), 340-344.

[29] Meng, F., & Demeter, D. (2023). Sentiment analysis with adaptive multi-head attention in Transformer. *arXiv preprint arXiv:2310.14505*.

[30] Manijeh Razeghi, Arash Dehzangi, Donghai Wu, Ryan McClintock, Yiyun Zhang, Quentin Durlin, Jiakai Li, and Fanfei Meng. Antimonite-based gap-engineered type-ii superlattice materials grown by mbe and mocvd for the third generation of infrared imagers. In Infrared Technology and Applications XLV, volume 11002, pages 108–125. SPIE, 2019.

[31] Meng, F., Zhang, L., Chen, Y., & Wang, Y. (2023). FedEmb: A Vertical and Hybrid Federated Learning Algorithm using Network And Feature Embedding Aggregation. *arXiv preprint arXiv:2312.00102*.

[32] Meng, F., Zhang, L., Chen, Y., & Wang, Y. (2023). Sample-based Dynamic Hierarchical Transformer with Layer and Head Flexibility via Contextual Bandit. *Authorea Preprints*.

[33] Meng, Fanfei, and Chen-ao Wang. "A Dynamic Interactive Learning Interface for Computer Science Education: Programming Decomposition Tool." *Authorea Preprints* (2023).

[34] Chang Ling, Chonglei Zhang, Mingqun Wang, Fanfei Meng, Luping Du, and Xiaocong Yuan, "Fast structured illumination microscopy via deep learning," Photon. Res. 8, 1350-1359 (2020)
[35] Meng, Fanfei, Lalita Jagadeesan, and Marina Thottan. "Model-based reinforcement learning for service mesh fault resiliency in a web application-level." *arXiv preprint arXiv:2110.13621* (2021).
[36] Meng, F., Wang, Y., Wang, X., & Xie, C. (2023). Optimizing the Passenger Flow for Airport Security Check. *Authorea Preprints*.
[37] Chen, Jin-Jin, et al. "A dataset of diversity and distribution of rodents and shrews in China." *Scientific Data* 9.1 (2022): 304
[38] Meng, F., Wang, Y., Zhang, L., Zhao, Y., & Demeter, D. (2023). Joint Detection Algorithm for Multiple Cognitive Users in Spectrum Sensing. *arXiv preprint arXiv:2311.18599*.
[39] Tomoumi Takase, Satoshi Oyama, and Masahito Kurihara. Effective neural network training with adaptive learning rate based on training loss. Neural Networks, 101:68–78, 2018.
[40] Raphael Tang, Yao Lu, Linqing Liu, Lili Mou, Olga Vechtomova, and Jimmy Lin. Distilling taskspecific knowledge from bert into simple neural networks, 2019.
[41] Karen Ullrich, Edward Meeds, and Max Welling. Soft weight-sharing for neural network compression, 2017. 12 Ashish Vaswani, Noam Shazeer, Niki Parmar, Jakob Uszkoreit, Llion Jones, Aidan N. Gomez, Lukasz Kaiser, and Illia Polosukhin. Attention is all you need, 2017.
[42] Elena Voita, David Talbot, Fedor Moiseev, Rico Sennrich, and Ivan Titov. Analyzing multi-head self-attention: Specialized heads do the heavy lifting, the rest can be pruned, 2019.
[43] Bo Wang, Minghui Qiu, Xisen Wang, Yaliang Li, Yu Gong, Xiaoyi Zeng, Jun Huang, Bo Zheng, Deng Cai, and Jingren Zhou. A minimax game for instance based selective transfer learning. In Proceedings of the 25th ACM SIGKDD International Conference on Knowledge Discovery Data Mining, KDD '19, pp. 34–43, New York, NY, USA, 2019. Association for Computing Machinery. ISBN 9781450362016. doi: 10.1145/3292500.3330841. URL https://doi.org/10.1145/3292500.3330841.
[44] Yingfei Wang, Hua Ouyang, Chu Wang, Jianhui Chen, Tsvetan Asamov, and Yi Chang. Efficient ordered combinatorial semi-bandits for whole-page recommendation. In Proceedings of the ThirtyFirst AAAI Conference on Artificial Intelligence, AAAI'17, pp. 2746–2753. AAAI Press, 2017.
[45] Licheng Xiao, Hairong Wang, and Nam Ling. Image compression with deeper learned transformer. In 2019 Asia-Pacific Signal and Information Processing Association Annual Summit and Conference (APSIPA ASC), pp. 53–57, 2019. doi: 10.1109/APSIPAASC47483.2019.9023342.
[46] Li Zhang, Liang Guo, Hongli Gao, Dawei Dong, Guoqiang Fu, and Xin Hong. Instancebased ensemble deep transfer learning network: A new intelligent degradation recognition method and its application on ball screw. Mechanical Systems and Signal Processing, 140:106681, 2020. ISSN 0888-3270. doi: https://doi.org/10.1016/j.ymssp.2020.106681. URL https://www.sciencedirect.com/science/article/pii/S0888327020300674.
[47] Xiang Zhang, Junbo Zhao, and Yann LeCun. Character-level convolutional networks for text classification, 2016.
[48] Barret Zoph and Quoc V. Le. Neural architecture search with reinforcement learning, 2017